SCIENCE CHINA
Chemistry

•ARTICLES•

August 2023 Vol.66 No.8: 2283–2291
https://doi.org/10.1007/s11426-023-1645-x

Redox-neutral *ipso*/*ortho* alkenylcyanation of (hetero)arylboronic acid enabled by 1,4-rhodium migration and fragmentation

Chenxia Guo, Donghui Xing, Huanfeng Jiang & Liangbin Huang*

The State Key Laboratory of Pulp and Paper Engineering, School of Chemistry and Chemical Engineering, Key Laboratory of Functional Molecular Engineering of Guangdong Province, South China University of Technology, Guangzhou 510640, China

Received April 3, 2023; accepted May 23, 2023; published online July 26, 2023

A mild, chemoselective, redox-neutral *ipso*/*ortho* alkenylcyanation of arylboronic acids with homopropargylic malononitriles *via* 1,4-rhodium migration and fragmentation is reported. A variety of 2-vinyl arylnitriles are obtained in good yields (51 examples, ava. 69% yields) through this strategy, which is characterized by its broad substrate scope, great functional group tolerance, and mild conditions. Mechanism studies indicate that the fragmentation is temperature dependent. The primary asymmetric exploration for the non-fragmentation product already shows promising results. The separation of the two cyano groups of homopropargylic malononitriles results in the formation of aromatic nitrile and aliphatic nitrile in one molecule, which enables the further transformations of the products.

1, 4-rhodium migration, alkenylcyanation, cyano transfer, malononitriles

Citation: Guo C, Xing D, Jiang H, Huang L. Redox-neutral *ipso*/*ortho* alkenylcyanation of (hetero)arylboronic acid enabled by 1,4-rhodium migration and fragmentation. *Sci China Chem*, 2023, 66: 2283–2291, https://doi.org/10.1007/s11426-023-1645-x

1 Introduction

Arylboronic acids and their derivatives are widely accessible and useful organic reagents, which have been extensively applied for carbon–carbon and carbon–heteroatom bond formations at the *ipso*-position with or without transition metal catalysis (Figure 1, left) [1,2]. Beyond any doubt, the pursuit of an alternative methodology to achieve the *ipso*/*ortho*-difunctionalization of arylboronic acids might constitute without considering the practicality and conceptuality, a worthwhile endeavor for organic synthesis (Figure 1, right).

The key to achieving the *ipso*/*ortho*-difunctionalization of arylboronic acids is introducing the metal catalyst into the *ortho*-position of the arylboronic acids. Miura and coworkers [3] utilized the merry-go-round strategy to fulfill the multiple alkylations of arylboronic acids with a strained alkene. However, this elegant protocol was limited in synthetic applications due to the strict restriction of alkenes substrates. Subsequently, the alkynes as the coupling partners were employed to achieve the *ipso*/*ortho*-difunctionalization of arylboronic acids (Figure 2a). Generally, the vinyl-M^n species **I**, generated by transmetallation and alkyne insertion, underwent the C–H activation to form the 5-membered cyclometallation intermediate **II** or proceeded the 1,4-metal migration to the *ortho*-position of arylboronic acid to access the intermediate **III**. These species were trapped by another molecule of alkyne or an intramolecular electrophilic site respectively to obtain the annulated products (Figure 2a). Since Hayashi's seminal work [4] of rhodium-catalyzed difunctionalization of arylboronic acids with two molecular of symmetric internal alkynes to produce the annulated derivatives, significant efforts have been made to unlock the cyclic *ipso*/*ortho*-difunctionalization of arylboronic acids (Figure 2a) [5,6]. Recently, Zhang and Zhou *et al*. [7] respectively reported an elegant Pd/norbornene (NBE) cata-

*Corresponding author (email: huanglb@scut.edu.cn)

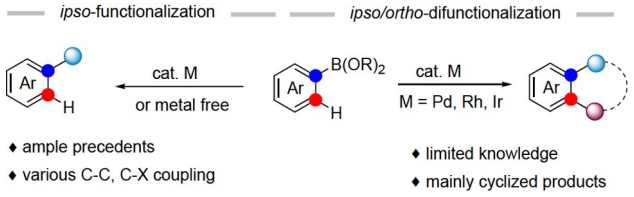

Figure 1 Transformations of the arylboronic acids (color online).

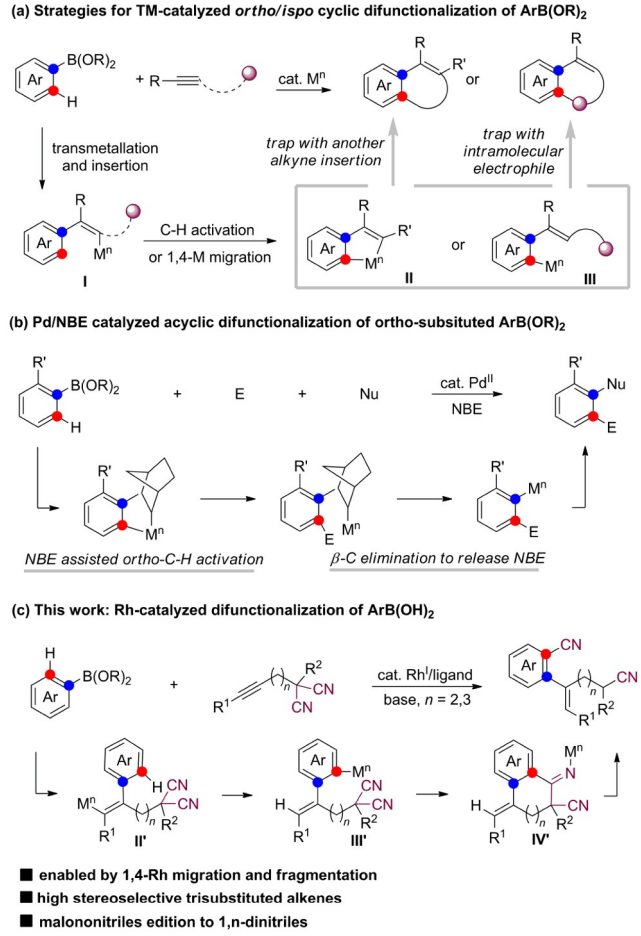

Figure 2 Transition metal-catalyzed *ipso*/*ortho* difunctionalization of arylboronic acid (color online).

lyzed boronic Catellani-type reaction, which expended the toolbox of difunctionalization of arylboronic acids to access various acyclic products (Figure 2b). However, those transformations were restricted to *ortho*-substituted arylboronic acids and required non-negligible amounts of norbornene.

Inspired by the recent C–CN activation of malononitrile derivatives *via* addition and fragmentation [8], we wondered whether a new catalytic blueprint could be designed *via* a cascade process based on a 1,4-Rh migration and fragmentation [6f,6h,6i], thus might complete a formal alkenylcyanation of arylboronic acids to construct functionalized *ortho*-vinyl arylnitriles (Figure 2c).

At the outset of the investigations, however, it was unclear whether this strategy could be implemented, as: (1) the regioselectivity of migratory insertion into the alkyne could occur as designed; (2) the aryl-Rh species directly reacted with the malononitrile site rather than inserted into the C–C triple bond [8b]; and (3) chemo-selectivity was another issue because the competitive protonation at the nitrogen center of intermediate **IV**' to form cyclic product instead of fragmentation to achieve the cyano transfer could be possible [9]. We recognized that, if successful, such 1,4-metal migration and fragmentation scenario might offer a new mode in the acyclic difunctionalization of arylboronic acids. Herein, we report the successful realization of this goal. This protocol is characterized by its excellent regio- and chemo-selectivity, mild conditions, and wide substrate scope.

2 Results and discussion

Our investigations began by evaluating the alkenylcyanation of phenylboronic acid **1a** with homopropargylic malononitrile **2a** in the presence of 5 mol% $RhCl(PPh_3)_3$ (Table 1). After considerable optimization (details see Tables S1–S10, Supporting Information online), when 10 mol% BINAP was applied as the ligand, the desired product **3a** was obtained in 49% yield (entry 1). As expected, the nature of the ligand had a non-negligible impact on reactivity. TFP could dramatically improve the yield to 90%, while DPPB as the ligand directly shut down the reactivity (entries 2 and 3). As shown in entries 3 and 4, excellent yields of **3a** were obtained when non-polar solvents, such as dioxane and toluene, were utilized as the solvent. The polar and coordinative solvent DMF gave no desired product (entry 5). Likewise, the nature of the base also had a significant effect on this transformation. Potassium carbonate was an excellent base for this reaction; however, no desired product was detected when KF was employed as the base (entries 6 and 7). Finally, a slight improvement in yield was found when the reaction temperature was decreased to 60 °C (entry 8).

We turned our attention to exploring the generality of this protocol for arylboronic acids under two sets of optimized conditions A and B using 5 mol% $RhCl(PPh_3)_3$ and 2.5 mol% $[RhCl(cod)]_2$ catalysts, respectively (details see Supporting Information online). As shown in Figure 3, a variety of substituents at the *para*-position of the arylboronic acids were well tolerated. The substrates bearing electron-donating substituents such as –Me, –OMe (**3b** and **3c**), electron-withdrawing groups such as $–OCF_3$, –Ph, –CN, $–CF_3$, –F, –CHO, –Ac or $–CO_2Me$ (**3d**–**3k**) were all converted into the corresponding products in moderate to excellent yields. Notably, the electrophilic functional groups, including nitrile, aldehyde, ketone, and ester, were well compatible with those transformations [10]. Those reactions worked well for aromatic boronic acids bearing primary and

Table 1 Optimization of the reaction conditions [a)]

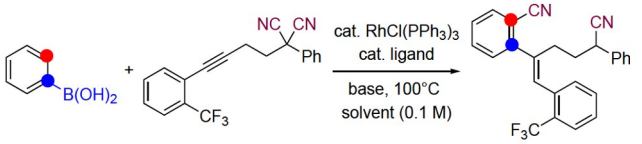

1a (0.15 mmol) **2a** (0.1 mmol) **3a**

Entry	Ligand [b)]	Base	Solvent	Yield [c)] (%)
1	BINAP	K_3PO_4	dioxane	49
2	DPPB	K_3PO_4	dioxane	0
3	TFP	K_3PO_4	dioxane	90
4	TFP	K_3PO_4	toluene	91
5	TFP	K_3PO_4	DMF	0
6	TFP	K_3CO_3	toluene	85
7	TFP	KF	toluene	0
8	TFP	K_3PO_4	toluene	94 (82) [d)]

a) Reaction conditions: **1a** (0.15 mmol, 1.5 equiv.), **2a** (0.10 mmol, 1.0 equiv.), base (0.20 mmol, 2 equiv.), $RhCl(PPh_3)_3$ (5.0 mol%), ligand (10 mol%), solvent (0.10 M, 1 mL) under 100 °C. b) TFP is tri(furan-2-yl) phosphane, DPPB is 1,4-bis(diphenylphosphanyl)butane. c) Corrected gas chromatograph (GC) yields were determined by using do-decane as an internal standard. d) 60 °C instead of 100 °C. Isolated yield is in the parentheses.

secondary amides at the *para*-position (**3l** and **3m**). Furthermore, the structure of **3m** was further confirmed by single-crystal X-ray analysis. It was clearly proved that the cyano group was transferred into the *ortho*-position of arylboronic acid. Interestingly, the chemoselective cyano-transfer product **3n** was obtained in moderate yield even in the presence of terminal styrene moiety [11]. For *meta*-substituted arylboronic acids (**3o** and **3p**), the cyano-transfer occurred selectively at the less steric hindered position, that was due to the 1,4-rhodium migration occurring at the less steric hindered position. Next, the *ortho*-fluoride substituted arylboronic acid was transformed into the 1,2,3-trisubstituted aromatic product **3q** in 76% yield. Multi-substituted arylboronic acid was also the suitable substrate (**3r**). When 2-naphthaleneboronic acid was utilized as the substrate, the cyano group was transferred into the 3-position of naphthalene in excellent yield (**3s**). Moreover, 1-naphthaleneboronic acid, which has large steric hindrance, was less reactive, and the desired product **3t** was still obtained in 57% yield. Then, it was found that alkenylcyanation of the heteroarylboronic acids, containing quinoline, benzothiophene, and dibenzofuran boronic acids, proceeded smoothly to afford the desired products in moderate to good yields (**3u**–**3w**). As expected, the fused-ring aromatic boronic acids were compatible with those transformations (**3x** and **3y**), which might have potential applications in organic light-emitting diodes [12].

Next, we explored the scope of homopropargylic malononitriles, and the results were summarized in Figure 4. In order to control the regioselectivity of alkynes migration (vide infra), the aryl group required an *ortho*-substituent, possibly due to the need for steric hindrance to differentiate the two sides of the alkyne [6a–6c,6e,6f]. As shown in Figure 4, various *ortho*-aryl substituted homopropargylic malononitriles were well tolerated and transformed into the corresponding products (**4a**–**4e**) in moderate to good yields. Fortunately, when the aryl group had a cyano group at the *para*-position, the desired product **4f** was also obtained in 43% yield, probably due to the electronic effect of the cyano group to control the regioselectivity of the alkyne insertion step. To our delight, electron-deficient heteroaryl substituted alkynes such as pyridine and quinoline (**4g** and **4h**) were well tolerated in those transformations.

Furthermore, we turned our attention to exploring the influence of various substituents at the α-position of the homopropargylic malononitriles. As expected, a wide range of aryl substituents, including various functional groups at the *para*-position, such as 4-methoxy (**4i**), 4-phenyl (**4j**), and 4-fluoro (**4k**) were well compatible with those transformations. The electron-withdrawing ester group at the *meta*-position was converted into the desired product in 72% yield (**4l**). Though the *ortho*-methoxyl group increased the steric hindrance, the desired product **4m** was also obtained in 46% yield. The multi-substituted aryl group with various substituents reacted smoothly to give the corresponding product **4n** in 66% yields. The 1-naphthalene group was tolerated, affording the desired product **4o** in 44% yields. Besides the aryl substituents at the α-position of homopropargylic malononitriles, the vinyl substituents were tolerated under the standard conditions (**4p** and **4q**).

Next, we explored the effect of less reactive benzylic substituents at the α-position of malononitriles (Figure 5) [9a–9d]. As expected, a mixture of products, cyano transfer product **4r** and cyclic product **5a** were obtained in a ratio of 3:1 under 100 °C. The cyclic product **5a** was obtained through competitive protonation instead of β-carbon elimination (*vide infra*) [9a–9c,13]. Fortunately, we could tune the selectivity *via* temperature control. As shown in Figure 5, when **2s** was utilized as a substrate, the annulated product **5a** was obtained as the sole product at 40 °C. When the temperature was gradually increased to 140 °C, the annulated product **5a** was totally suppressed, and the cyano transfer product **4r** was afforded in 78% yield. It was worth to mention that the 2-phenyl pyridine moiety of **2s** did not inhibit this transformation. The different reactivity between benzyl- and aryl-substituted substrates could be explained by the acidity of the α-position of the malononitrile, which droves the β-elimination to a degree.

With the optimal conditions in hand, we explored the scope of various benzylic-substituted homopropargylic malononitriles (Figure 6). Homopropargylic malononitriles with several benzylic substituents were all suitable substrates (**4s**–**4w**). Heterocycles, such as furyl (**4x**) and thienyl (**4y**), were

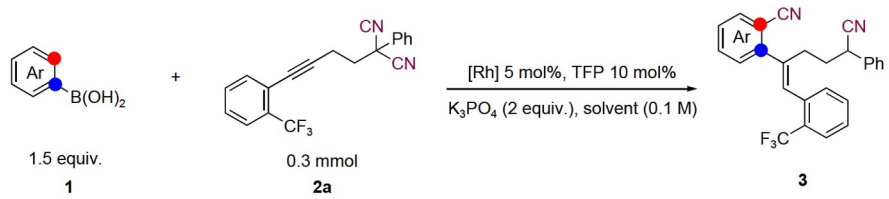

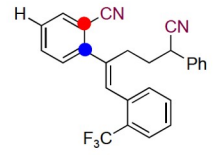
3a, 82% [A]

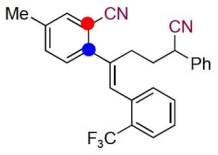
3b, 72% [A]

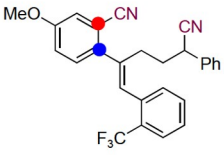
3c, 61% [A]

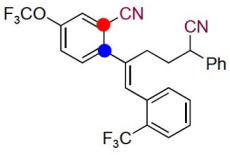
3d, 70% [B]

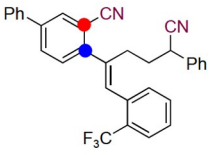
3e, 84% [B]

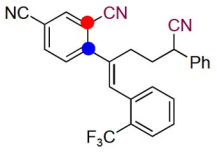
3f, 70% [B]

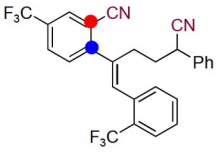
3g, 92% [B]

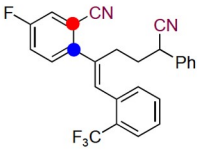
3h, 59% [B]

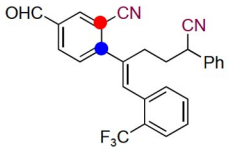
3i, 58% [B]

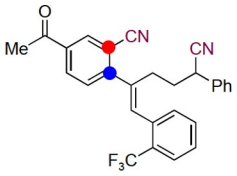
3j, 68% [A]

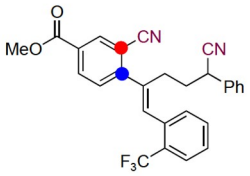
3k, 70% [B]

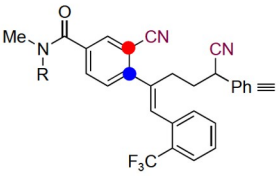
R = H, **3l**, 57% [B]
R = Me, **3m**, 76% [B]

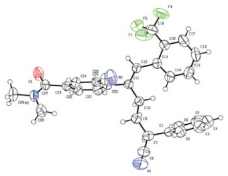
single-crystal X-ray of **3m** (**CCDC:** 2125921)

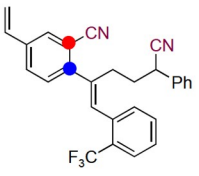
3n, 46% [B]

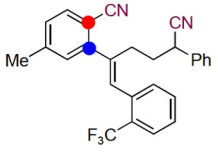
3o, 94% [A]

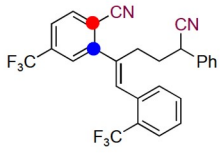
3p, 64% [B]

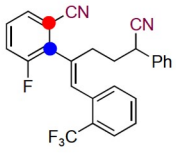
3q, 76% [B]

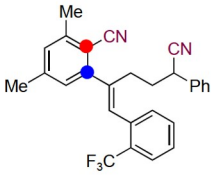
3r, 69% [B]

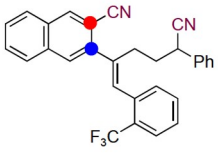
3s, 90% [A]

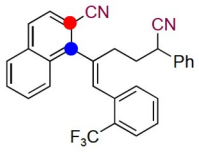
3t, 57% [A]

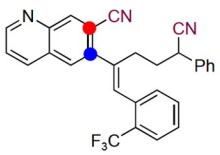
3u, 80% [B]

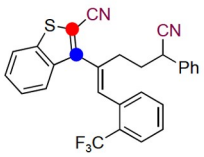
3v, 44% [B]

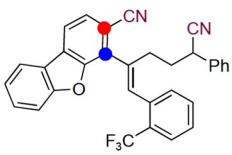
3w, 87% [B]

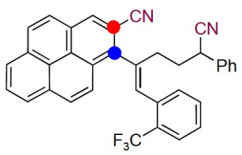
3x, 78% [B]

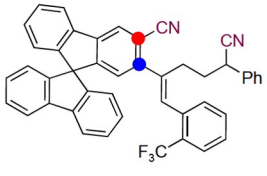
3y, 74% [B]

Figure 3 The scope of arylboronic acids. Reaction condition A: $RhCl(PPh_3)_3$ (5 mol%), toluene (0.1 M) at 60 °C in N_2 for 6 h. Reaction condition B: $[RhCl(cod)]_2$ (2.5 mol%), dioxane (0.1 M) at 100 °C in N_2 for 20 h (color online).

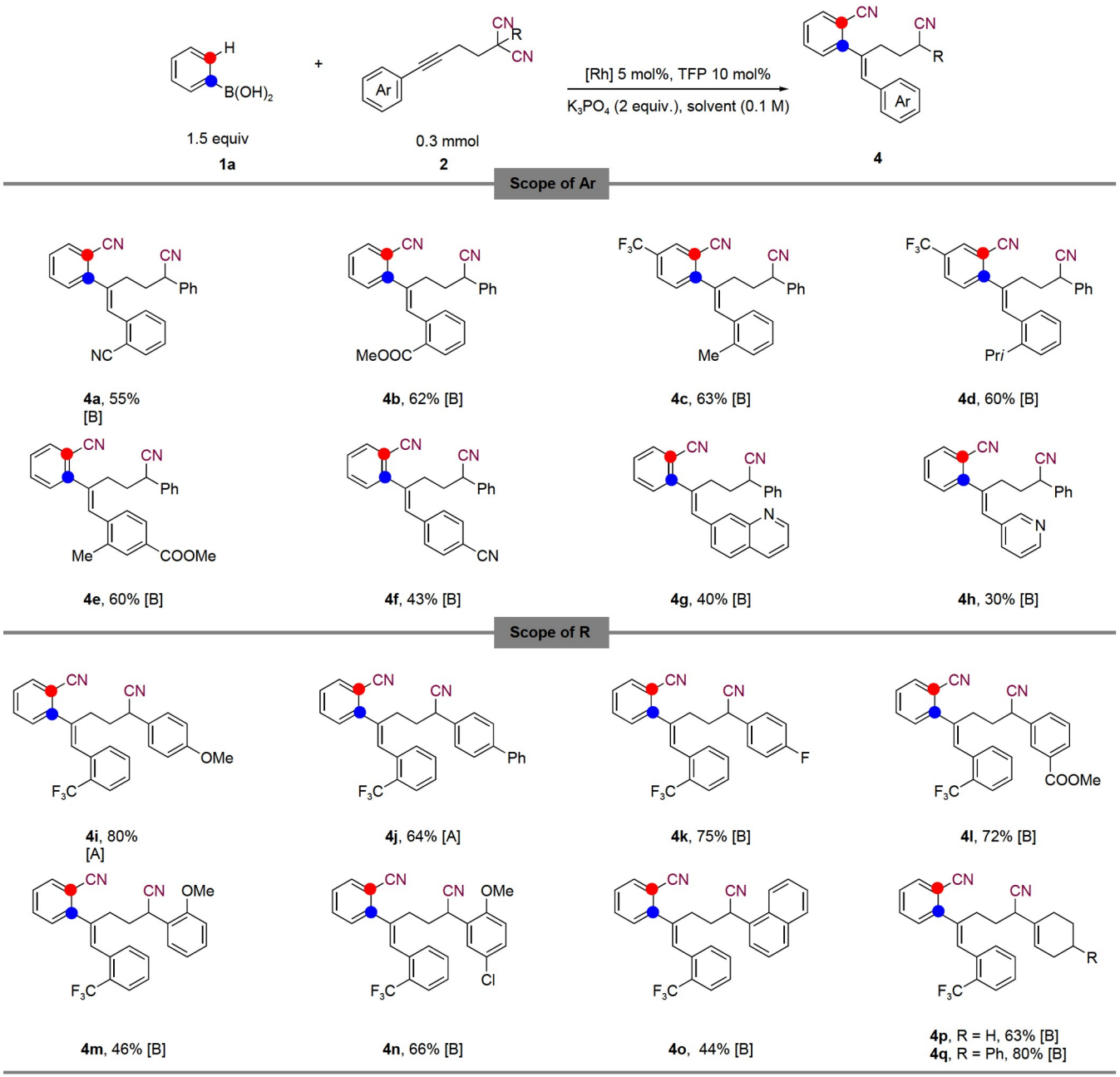

Figure 4 Scope of substituted malononitriles. Reaction condition A: $RhCl(PPh_3)_3$ (5 mol%), toluene (0.1 M) at 60 °C in N_2 for 6 h. Reaction condition B: $[RhCl(cod)]_2$ (2.5 mol%), dioxane (0.1 M) at 100 °C in N_2 for 20 h (color online).

also accommodated in this process. The carbon chain length for the cyano transfer process was also surveyed (**4z, 4aa**). The substrate with a longer alkyne-malononitrile tethered, unsurprisingly resulted in a lower yield, as it would require an 8-membered-ring intermediate. The substrate with an even longer carbon chain was unsuitable at this stage. However, substrates with a shorter tether length did not react because the steric resistance at both ends of the alkyne increased in this case, and the process of migration insertion was challenging to occur.

After that, we also examined the scope of the reaction to synthesize cycloheptanones at 40 °C. It was found that malononitriles with several benzylic substituents, including benzyl (**5b**) and 4-phenoxy benzyl (**5c**–**5e**), worked smoothly, producing the corresponding cycloheptanone products in good yields. Besides, homopropargylic malononitriles with alkyl substituents were proven to be competent substrates for those reaction conditions, giving the α-alkyl substituted cycloheptanone (**5f**) in good yield. We explored the asymmetric synthesis of **5b** by trying several chiral ligands, and a promising result was obtained, 70% yield with 55% ee (Table S11).

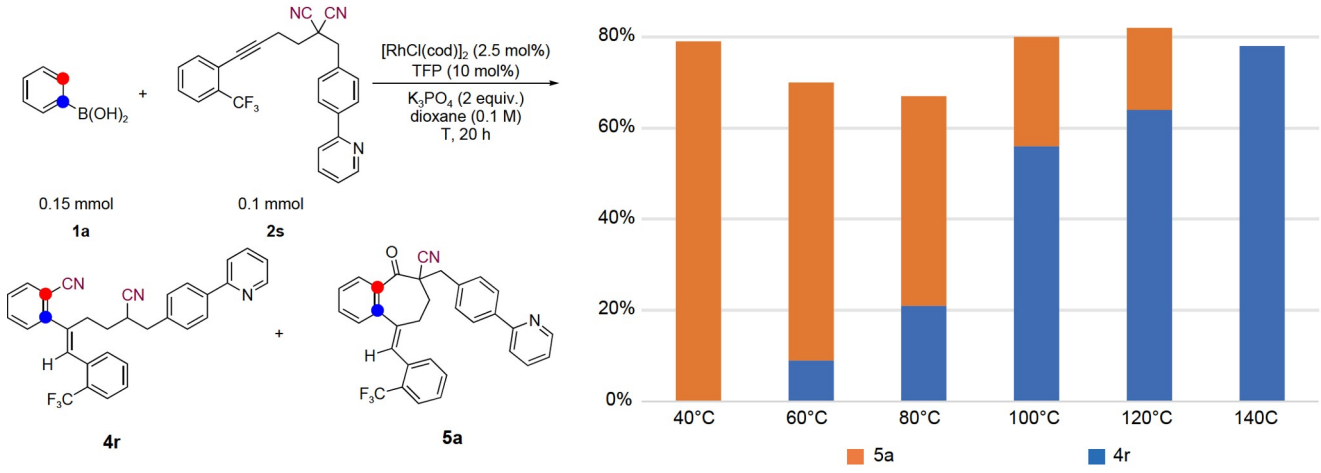

Figure 5 Temperature-dependent fragmentation of benzylic substituted malononitriles (color online).

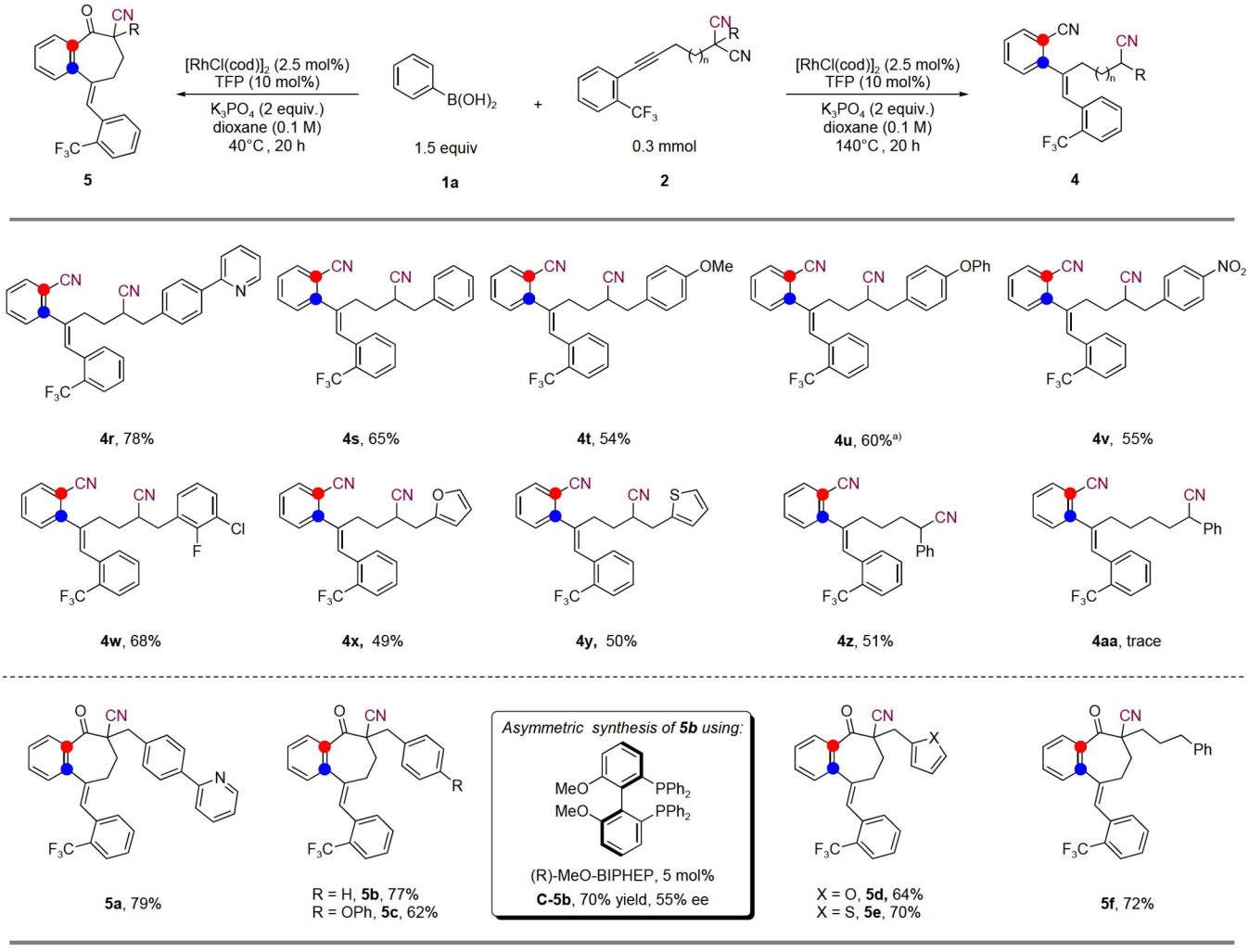

Figure 6 Substrate scope of benzylic substituted malononitriles. Unless otherwise noted, all reactions were run with **1a** (0.45 mmol), **2** (0.3 mmol), [RhCl(cod)]$_2$ (2.5 mol%), TFP (10 mol%), K_3PO_4 (2 equiv.), and dioxane (0.1 M) at 140 or 40 °C in N_2 for 20 h. a) 160 °C instead of 140 °C (color online).

To gain insight into the mechanism of those transformations, we carried out some control experiments, and the results were outlined in Figure 7. Switching one cyano group of malononitrile into the ester group, we observed only a

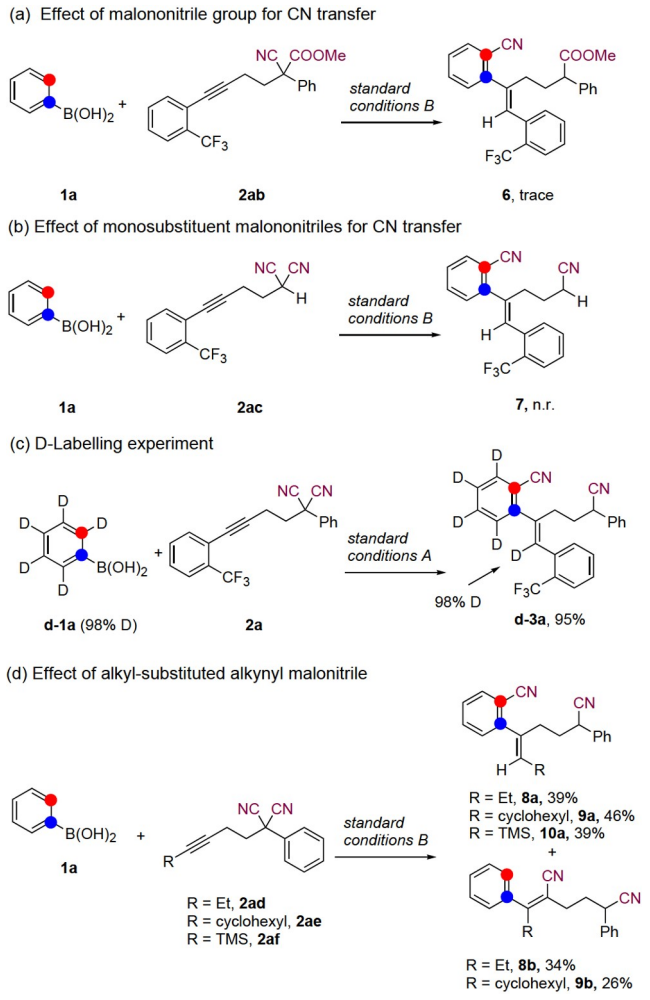

Figure 7 Control experiments (color online).

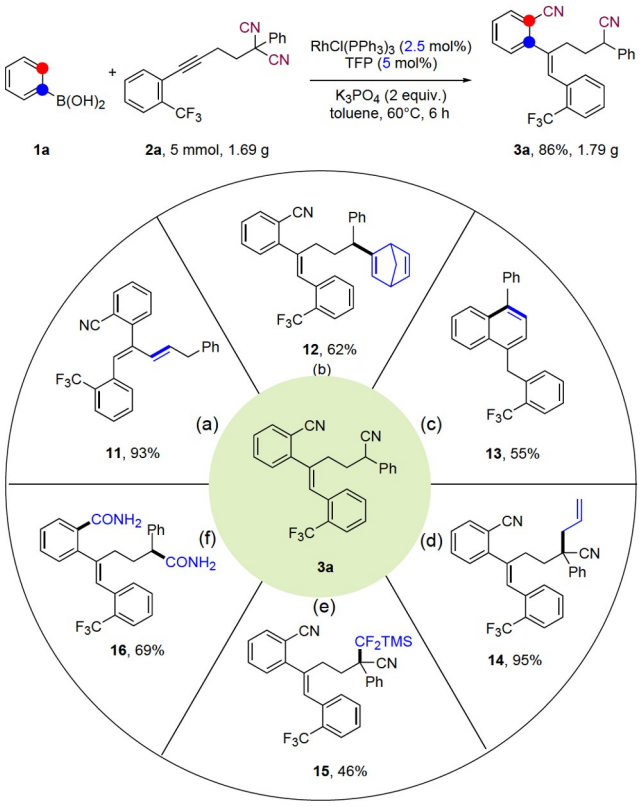

Figure 8 Gram-scale reaction and synthetic applications of 1,*n*-dinitrile. Reaction conditions: (a) $Pd_2(dba)_3$ (2.5 mol%), CyJohnphos (10 mol%), $AlMe_2Cl$ (0.2 equiv.), styrene (5.0 equiv.), toluene, 100 °C, N_2, 16 h; (b) $Ni(cod)_2$ (5 mol%), DPEphos (5 mol%), $AlMe_2Cl$ (0.2 equiv.), 2,5-norbornadiene (1.1 equiv.), toluene, r.t., N_2, 16 h; (c) $Ni(cod)_2$ (5 mol%), DPEphos (5 mol%), $AlMe_2Cl$ (0.2 equiv.), oct-4-yne (1.1 equiv.), toluene, 80 °C, N_2, 16 h; (d) LDA (1.2 equiv.), allyl bromide (1.2 equiv.), tetrahydrofuran (THF), 0 °C, N_2, 10 h; (e) ^{n}Bu-Li (1.2 equiv.), $TMSCF_2Br$ (3.0 equiv.), toluene, r.t., 5 h; (f) 30% H_2O_2 (0.05 M), K_2CO_3 (2 equiv.), dimethyl sulfoxide (DMSO), r.t., 16 h (color online).

trace amount of the corresponding cyano-transfer product **6** and a complicated mixture was obtained [8b]. That indicated that the malononitrile moiety was crucial for those reactions (Figure 7a) [8,14]. We investigated whether the malononitrile with a monosubstituent could participate in the reaction, and it turned out that the reaction could not occur. This demonstrate that substrate with a quaternary carbon is essential for this transformation (Figure 7b). Furthermore, the D-labeling experiment of **d-1a** was conducted (Figure 7c). The deuterium at one of the *ortho*-positions of **d-1a** was quantitatively shifted to the alkenyl position, demonstrating the 1,4-rhodium(I) migration of this transformation. Ethyl-substituted homopropargylic malononitrile **2ad** was explored as a substrate for cyano transfer. The regioselectivity of alkyne migratory insertion into the Ar-Rh species was significantly decreased. The expected cyano transfer product **8a** was obtained in 39% isolated yield and 34% of **8b**, which was accessed *via* direct cyano transfer without 1,4-Rh migration [6i,15]. The regioselectivity of alkyne migratory insertion improved when using cyclohexyl-substituted homopropargylic malononitrile **2ae**, delivering the corresponding products (**9a** and **9b**) in 72% total yields with 1.7:1 selectivity. Only cyano transfer product with 1,4-Rh migration (**10a**) was obtained from the TMS-substituted homopropargylic malononitrile **2af** with 39% yield (Figure 7d).

To evaluate the practicability of the strategy, we carried out a gram-scale reaction. At a lower catalyst loading, the reaction on a 5 mmol scale delivered 1.79 g of the desired product **3a** in 86% yield (Figure 8, top). The synthetic utility of our protocol was further highlighted in Figure 8. The separated two cyano groups could be utilized as a handle for subsequent manipulation. Firstly, the activation and transformation of the benzylic C–CN bond were evaluated. In the presence of styrene as an HCN acceptor, a retro-hydrocyanation reaction followed by isomerization to furnish 1,3-diene product **11** in 93% yield (Figure 8a) [16]. Interestingly, the C–CN activation and coupling of 2,5-norbornadiene gave the Heck-type product **12** in 62% yield (Figure 8b) [17]. Surprisingly, utilization of oct-4-yne as HCN acceptor, **3a** was transformed into the naphthalene **13** through double

C–CN bond activation and cyclization (Figure 8c, details see Figure S1, Supporting Information online). Furthermore, we utilized the acidity of α-C–H bond of benzylic cyanide to couple with allylic bromide [18] and $TMSCF_2Br$ [19] to give the corresponding allylation product **14** in excellent yield and siladifluoromethylated product **15** in moderate yield (Figure 8d, e). In addition, both aryl and benzyl nitrile could be hydrated to afford amides **16** in 69% yield (Figure 8f) [20].

Based on the results of the control experiments and previous reports [6b,6f,8b], we proposed the following mechanism for those transformations (Figure 9). First, an aryl-rhodium species **II** was generated by transmetallation of the aryl boronic acid with the rhodium catalyst **I**. Migratory insertion of the alkyne **2** into Ar-Rh species occurred to give alkenyl-Rh species **III**, which underwent 1,4-migration [3,4,21]. The resulting aryl-Rh intermediate **IV** coordinated with one cyano group and then inserted into the cyano group to generate the intermediate **V**. Finally, β-C elimination and protonation of **VI** released product **3** and regenerated the rhodium catalyst. Competitive protonation of **V** generated the imine product, which was further hydrolyzed to yield the cycloheptanone derivative **5**.

3 Conclusions

In summary, we have developed a novel platform that streamlines the preparation of 2-vinyl arylnitriles from simple arylboronic acids with alkynyl malononitriles. This redox-neutral *ipso*/*ortho* alkenylcyanation of arylboronic acid is achieved by harnessing the 1,4-rhodium migration and fragmentation. Moreover, this method is characterized by its broad substrate scope, excellent functional group tolerance, and mild conditions. The mechanism studies indicate that the fragmentation is temperature-dependent, and the primary asymmetric exploration for the non-fragmentation product already shows promising results. The further asymmetric synthesis of these products is undertaken by our laboratory.

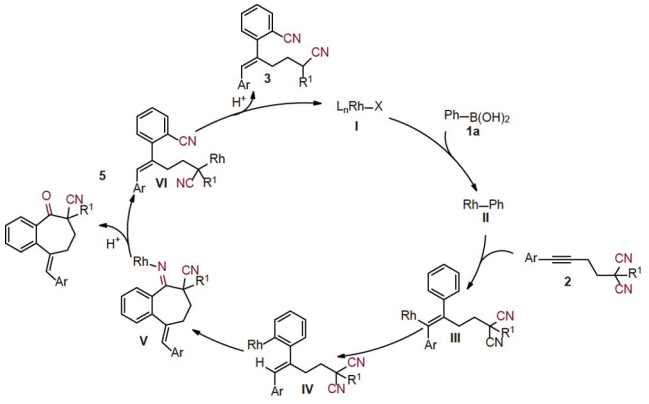

Figure 9 Plausible mechanism (color online).

Acknowledgements This work was supported by the National Natural Science Foundation of China (21971074), the Natural Science Foundation of Guangdong Province (2022A1515010660, 2021A1515220024), and Natural Science Foundation of GuangZhou (202102020982). We further thank Dr. H. Jiang for technical assiatance with IR, Prof. Daniel J. Weix for the discussion and helpful suggestions about this paper. Dr. Y. Zhao from Francool Technology (Shenzhen) Co. Ltd. is gratefully acknowledged for his help with the manuscript.

Conflict of interest The authors declare no conflict of interest.

Supporting information The Supporting Information is available online at http://chem.scichina.com and http://link.springer.com/journal/11426. The supporting materials are published as submitted, without typesetting or editing. The responsibility for scientific accuracy and content remains entirely with the authors.

1 (a) Hedouin G, Hazra S, Gallou F, Handa S. *ACS Catal*, 2022, 12: 4918–4937; (b) Corpas J, Mauleón P, Arrayás RG, Carretero JC. *ACS Catal*, 2021, 11: 7513–7551; (c) West MJ, Fyfe JWB, Vantourout JC, Watson AJB. *Chem Rev*, 2019, 119: 12491–12523; (d) Malapit CA, Bour JR, Brigham CE, Sanford MS. *Nature*, 2018, 563: 100–104; (e) Miyaura N, Suzuki A. *Chem Rev*, 1995, 95: 2457–2483

2 (a) Wang H, Jing C, Noble A, Aggarwal VK. *Angew Chem Int Ed*, 2020, 59: 16859–16872; (b) Roscales S, Csáky AG. *Chem Soc Rev*, 2020, 49: 5159–5177; (c) Wu P, Givskov M, Nielsen TE. *Chem Rev*, 2019, 119: 11245–11290; (d) Zhu C, Falck JR. *Adv Synth Catal*, 2014, 356: 2395–2410

3 Oguma K, Miura M, Satoh T, Nomura M. *J Am Chem Soc*, 2000, 122: 10464–10465

4 Hayashi T, Inoue K, Taniguchi N, Ogasawara M. *J Am Chem Soc*, 2001, 123: 9918–9919

5 (a) Kong W-, Finger LH, Oliveira JCA, Ackermann L. *Angew Chem Int Ed*, 2019, 58: 6342–6346; (b) Xu S, Chen K, Chen H, Yao J, Zhu X. *Chem Eur J*, 2014, 20: 16442–16447; (c) Karthikeyan J, Haridharan R, Cheng CH. *Angew Chem Int Ed*, 2012, 51: 12343–12347; (d) Fukutani T, Hirano K, Satoh T, Miura M. *J Org Chem*, 2011, 76: 2867–2874; (e) Fukutani T, Hirano K, Satoh T, Miura M. *Org Lett*, 2010, 11: 5198–5201

6 (a) Selmani A, Darses S. *Org Lett*, 2020, 22: 2681–2686; (b) Groves A, Sun J, Parke HRI, Callingham M, Argent SP, Taylor LJ, Lam HW. *Chem Sci*, 2020, 11: 2759–2764; (c) Selmani A, Darses S. *Org Lett*, 2019, 21: 8122–8126; (d) O'Brien L, Karad SN, Lewis W, Lam HW. *Chem Commun*, 2019, 55: 11366–11369; (e) Wang JX, Tan YX, Liao WW, Tian P, Lin GQ, Zhao Q. *Synlett*, 2018, 29: 1223–1228; (f) Claraz A, Serpier F, Darses S. *ACS Catal*, 2017, 7: 3410–3413; (g) Partridge BM, Solana González J, Lam HW. *Angew Chem Int Ed*, 2014, 53: 6523–6527; (h) Shintani R, Isobe S, Takeda M, Hayashi T. *Angew Chem Int Ed*, 2010, 49: 3795–3798; (i) Miura T, Sasaki T, Nakazawa H, Murakami M. *J Am Chem Soc*, 2005, 127: 1390–1391

7 (a) Chen S, Liu ZS, Yang T, Hua Y, Zhou Z, Cheng HG, Zhou Q. *Angew Chem Int Ed*, 2018, 57: 7161–7165; (b) Shi G, Shao C, Ma X, Gu Y, Zhang Y. *ACS Catal*, 2018, 8: 3775–3779; (c) Chen S, Wang P, Cheng HG, Yang C, Zhou Q. *Chem Sci*, 2019, 10: 8384–8389; (d) Wang P, Chen S, Zhou Z, Cheng HG, Zhou Q. *Org Lett*, 2019, 21: 3323–3327

8 (a) Mills LR, Graham JM, Patel P, Rousseaux SAL. *J Am Chem Soc*, 2019, 141: 19257–19262; (b) Malapit CA, Reeves JT, Busacca CA, Howell AR, Senanayake CH. *Angew Chem Int Ed*, 2016, 55: 326–330; (c) Reeves JT, Malapit CA, Buono FG, Sidhu KP, Marsini MA, Sader CA, Fandrick KR, Busacca CA, Senanayake CH. *J Am Chem Soc*,

2015, 137: 9481–9488
9 (a) Chen ZH, Sun RZ, Yao F, Hu XD, Xiang LX, Cong H, Liu WB. *J Am Chem Soc*, 2022, 144: 4776–4782; (b) Hu XD, Chen ZH, Zhao J, Sun RZ, Zhang H, Qi X, Liu WB. *J Am Chem Soc*, 2021, 143: 3734–3740; (c) Lu Z, Hu XD, Zhang H, Zhang XW, Cai J, Usman M, Cong H, Liu WB. *J Am Chem Soc*, 2020, 142: 7328–7333; (d) Malapit CA, Caldwell DR, Luvaga IK, Reeves JT, Volchkov I, Gonnella NC, Han ZS, Busacca CA, Howell AR, Senanayake CH. *Angew Chem Int Ed*, 2017, 56: 6999–7002; (e) Zhang X, Xie X, Liu Y. *Chem Sci*, 2016, 7: 5815–5820
10 (a) Yang J, Chen X, Wang Z. *Tetrahedron Lett*, 2015, 56: 5673–5675; (b) Korenaga T, Ko A, Uotani K, Tanaka Y, Sakai T. *Angew Chem Int Ed*, 2011, 50: 10703–10707; (c) Ueura K, Miyamura S, Satoh T, Miura M. *J Organomet Chem*, 2006, 691: 2821–2826
11 Lautens M, Roy A, Fukuoka K, Fagnou K, Martín-Matute B. *J Am Chem Soc*, 2001, 123: 5358–5359
12 Sasabe H, Kido J. *Chem Mater*, 2010, 23: 621–630
13 Ueura K, Satoh T, Miura M. *Org Lett*, 2005, 7: 2229–2231
14 Li H, Zhang S, Yu X, Feng X, Yamamoto Y, Bao M. *Chem Commun*, 2019, 55: 1209–1212
15 (a) Choi K, Park H, Lee C. *J Am Chem Soc*, 2018, 140: 10407–10411; (b) He ZT, Tian B, Fukui Y, Tong X, Tian P, Lin GQ. *Angew Chem Int Ed*, 2013, 52: 5314–5318; (c) Miura T, Shimada M, Murakami M. *J Am Chem Soc*, 2005, 127: 1094–1095; (d) Shintani R, Tsurusaki A, Okamoto K, Hayashi T. *Angew Chem Int Ed*, 2005, 44: 3909–3912; (e) Miura T, Shimada M, Murakami M. *Angew Chem Int Ed*, 2005, 44: 7598–7600
16 Fang X, Yu P, Prina Cerai G, Morandi B. *Chem Eur J*, 2016, 22: 15629–15633
17 Fang X, Yu P, Morandi B. *Science*, 2016, 351: 832–836
18 Chen C, Hou C, Chen P, Liu G. *Chin J Chem*, 2020, 38: 346–350
19 Aikawa K, Maruyama K, Honda K, Mikami K. *Org Lett*, 2015, 17: 4882–4885
20 Katritzky AR, Pilarski B, Urogdi L. *Synthesis*, 1989, 1989(12): 949–950
21 (a) Lu X, Huang Y. *Org Chem Front*, 2021, 8: 3008–3013; (b) Zhang SS, Hu TJ, Li MY, Song YK, Yang XD, Feng CG, Lin GQ. *Angew Chem Int Ed*, 2019, 58: 3387–3391; (c) Liu N, Yao J, Yin L, Lu T, Tian Z, Dou X. *ACS Catal*, 2019, 9: 6857–6863; (d) Ming J, Shi Q, Hayashi T. *Chem Sci*, 2018, 9: 7700–7704; (e) Partridge BM, Callingham M, Lewis W, Lam HW. *Angew Chem Int Ed*, 2017, 56: 7227–7232; (f) Callingham M, Partridge BM, Lewis W, Lam HW. *Angew Chem Int Ed*, 2017, 56: 16352–16356; (g) Ma S, Gu Z. *Angew Chem Int Ed*, 2005, 44: 7512–7517